Reliability Evaluation of Power Capacitors in a Wind Turbine System

Zhou, Dao; Blaabjerg, Frede

Published in:
APEC 2018 - 33rd Annual IEEE Applied Power Electronics Conference and Exposition

DOI (link to publication from Publisher):
10.1109/APEC.2018.8341570

Publication date:
2018

Document Version
Accepted author manuscript, peer reviewed version

Reliability Evaluation of Power Capacitors in a Wind Turbine System

Dao Zhou, and Frede Blaabjerg

Department of Energy Technology
Aalborg University, Aalborg, Denmark
zda@et.aau.dk; fbl@et.aau.dk

***Abstract* - With the increasing penetration of wind power, reliable and cost-effective wind energy production is of more and more importance. The doubly-fed induction generator based partial-scale wind power converter is still dominating in the existing wind farms. In this paper, the reliability assessment of power capacitors is studied considering the annual mission profile. According to an electro-thermal stress evaluation, the time-to-failure distribution of both the dc-link capacitor and ac-side filter capacitor is detailed investigated. Aiming for the system-level reliability analysis, a reliability block diagram is used to bridge the gap between the Weibull distribution based component-level individual capacitor and the capacitor bank. A case study of a 2 MW wind power converter shows that the lifetime is significantly reduced from the individual capacitor to the capacitor bank. Besides, the dc-link capacitor bank dominates the lifetime consumption.**

I. INTRODUCTION

With the increasing penetration of wind power during recent decades, the reliable and cost-effective wind energy production is of more and more importance [1]. In order to reduce the cost of the wind power generation, the power rating of the individual wind turbine is up-scaled to 8 MW and even above. However, the feedback of the wind turbine market indicates that the best-seller is still those rated around 2-3 MW, in which the Doubly-Fed Induction Generator (DFIG) is normally employed together with a partial-scale power electronic converters [2]. Another tendency of the wind power development is the popularity of the offshore wind farms, which pushes the wind turbine system to operate with reliable performance due to the high maintenance cost. Reliability and robustness of the system are closely related to its mission profile - the representation of all relevant conditions that the system will be exposed to in all of its intended application throughout its entire life cycle [3]. The failure may happen during the overlap of the strength and stress distribution, in which the stressor factors may appear due to the environmental loads (like thermal, mechanical, humidity, etc.), or the functional loads (such as usage profiles, electrical operation) [4].

The performance of power capacitor is complicated and highly affected by its operation conditions such as the voltage, current, frequency, and temperature. Many researchers have investigated the degradation of the electrolytic capacitors [5]-[8]. For instance, a real-time failure detection is developed for the changes of the ESR and capacitance of the capacitors [6]. Lifetime prediction models of electrolytic capacitors are established for the switch-mode power supplies and variable-frequency drivers [7]. However, few studies investigate the degradation effect on reliability evaluation considering the mission profile [8], and this paper develops the approach to evaluate the reliability of power capacitors used in power conversion stage. Moreover, it is a physics-of-failure approach from the component-level [9] to system-level reliability that integrates the electrical modeling, thermal modeling, Weibull distribution, and reliability block diagram.

This paper addresses the reliability assessment of the capacitors in a DFIG wind turbine system. Section II describes the basic design of dc-side and ac-side capacitors. Mission profile based lifetime estimation of individual capacitor is presented in Section III. Afterwards, Section IV investigates and compares the time-to-failure from the single capacitor to capacitor bank. The concluding remarks are drawn in last section.

II. DESIGN OF DC-SIDE AND AC-SIDE CAPACITORS

In the application of a wind power generation system, various types of the capacitor are selected in the power conversion stage. The aluminum electrolytic capacitors (Al-CAP) are normally used in the dc-side for energy storage, while the metalized polypropylene film capacitors (MPF-CAP) are generally applied in the ac-side featuring as harmonic filtering. The design and selection of the dc-side and ac-side capacitor banks will be described in this section.

The configuration of a 2 MW DFIG wind turbine system is shown in Fig. 1, where the back-to-back power converter is with the partial-scale power rating compared to the generator. The Al-CAP in the dc-link serves as the energy storage and power decouple, and the MPF-CAP in the grid-side filters out the current ripple introduced by the PWM switching pattern.

The selection of the dc capacitor C_{dc} is based on the balance of the energy exchange during the transient period [10],

$$C_{dc} \geq \frac{T_r \Delta P_{\max}}{2U_{dc}\Delta U_{\max}} \tag{1}$$

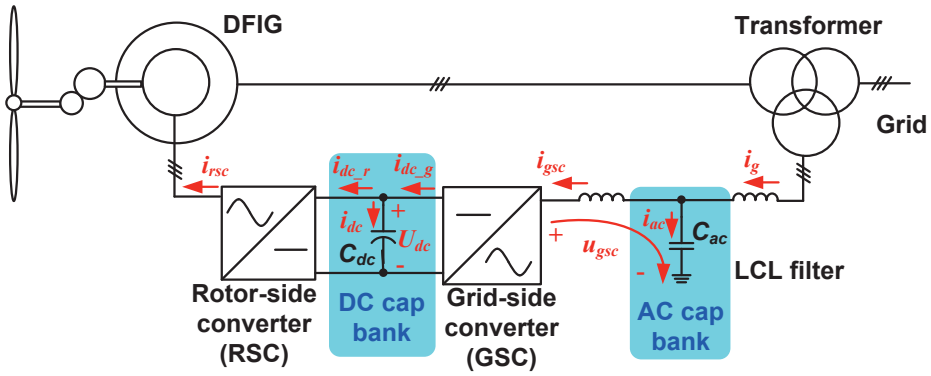

Fig. 1. DC and AC capacitor bank located in a doubly-fed induction generator wind turbine system.

where ΔP_{max} denotes the maximum variation of the output power, T_r denotes the control response time – a few modulation period, U_{dc} denotes the dc-link voltage, and ΔU_{max} denotes the maximum voltage variation.

Table I

PARAMETERS OF 2 MW DFIG SYSTEM

Rated power	2 MW
Operational range of rotor speed	1050-1800 rpm
Rated amplitude of phase voltage	563 V
Mutual inductance	2.91 mH
Stator leakage inductance	0.04 mH
Rotor leakage inductance	0.06 mH
Ratio of stator winding and rotor winding	0.369
Dc-link voltage	1050 V
Dc-link capacitor	20 mF
Grid-side inductor	125 μH
Converter-side inductor	125 μH
Ac-side filter capacitor	300 μF
Switching frequency	2 kHz

The parameters of the 2 MW DFIG system is listed in Table I. In order to achieve the high ride-through capability during utility voltage sag event, the capacitance of 20 mF is selected. Due to the limitation of the rated voltage, 72 pieces of 4700 μF/400V are selected – 4 in series and 18 in parallel [11].

The detailed design procedure of LCL filter is presented in [12], and the ac capacitance of 300 μF is designed according to 10% of absorbed reactive power at rated condition. As the delta connection is normally applied in practice, 100 μF is equivalent to use, which is consisted of 10 pieces of 10 μF/780V from the leading capacitor manufacturer [13].

III. LIFETIME ESTIMATION OF INDIVIDUAL CAPACITOR

In this section, based on the harmonic component of the dc-side and ac-side capacitors, their loss dissipation can be calculated at typical operation points. Then, the mission profile based thermal stress can be evaluated, which can serve to predict the operational lifetime.

As shown in Fig. 2, the dc-link current is observed at the rated power (wind speed at 12 m/s). It can be seen that the dominating frequency of the dc-link current is around 4 kHz and 8 kHz, where the switching frequency is set at 2 kHz. Since only the slip power flows through the dc-link, the amplitude of the harmonic component is mainly in line with the slip power.

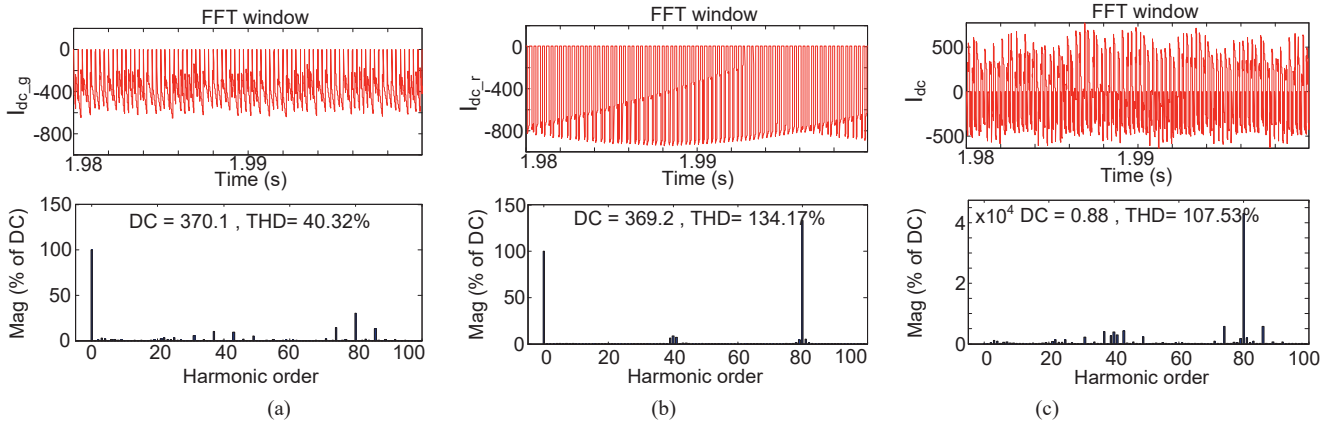

Fig. 2. Simulation result of dc-side current at wind speed of 12 m/s. (a) Dc-side current from the grid-side converter. (b) Dc-side current from the rotor-side converter. (c) Current of dc-link capacitor.

As shown in Fig. 3, the current through ac capacitor is simulated at the same conditions of the dc-link current. The amplitude of the fundamental current almost keeps unchanged due to the same grid voltage at various operation points. Moreover, the similar harmonic orders around switching frequency can be found as well.

According to the mission profile of the wind turbine system (e.g. wind speed and ambient temperature), the general procedure to calculate the B_{10} lifetime of the capacitors is shown in Fig. 4. It can be seen that only the Joule power loss is considered in the Al-CAP, but both the Joule power loss and dielectric power loss are taken into account in the MPF-CAP.

The lifetime model of the capacitor from the leading manufacturer is expressed as,

$$L_x = L_r \cdot \left(\frac{V_r}{V_x}\right)^{-n_1} \cdot 2^{\frac{T_r - T_x}{n_2}} \tag{2}$$

where L_x denotes the hours to failure at the applied voltage V_x and operational core temperature T_x, and L_r denotes the hours to failure at the rated voltage V_r and upper categorized temperature T_r. n_1 and n_2 are affecting coefficients of the voltage and temperature. It is noted that n_2 equals to 10, while the n_1 equals to 1 for the Al-CAP and 7 for the MPF-CAP due to their different degradation mechanisms [14].

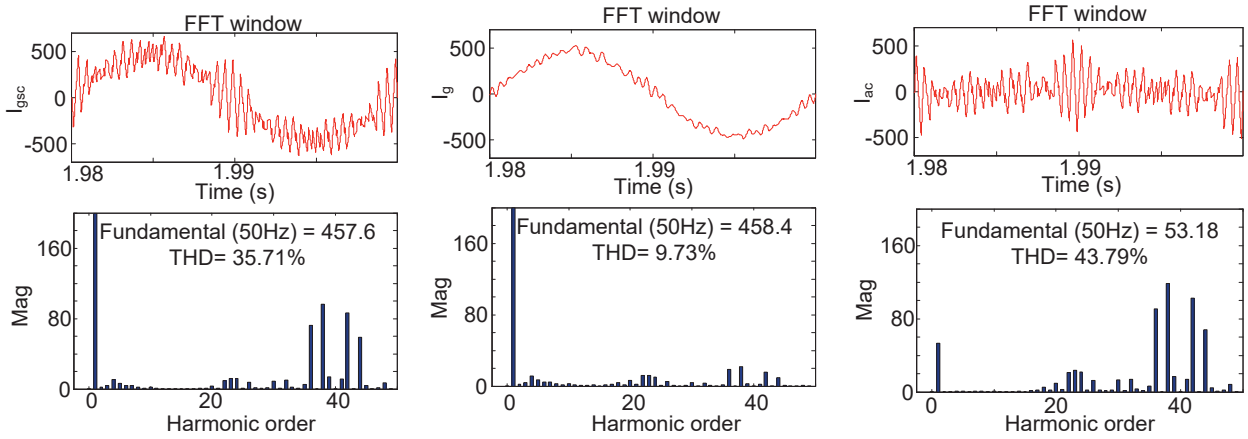

Fig. 3. Simulation result of grid-side converter at wind speed of 12 m/s. (a) Output phase voltage. (b) Grid-side converter current. (c) Grid current. (d) Ac-side capacitor current.

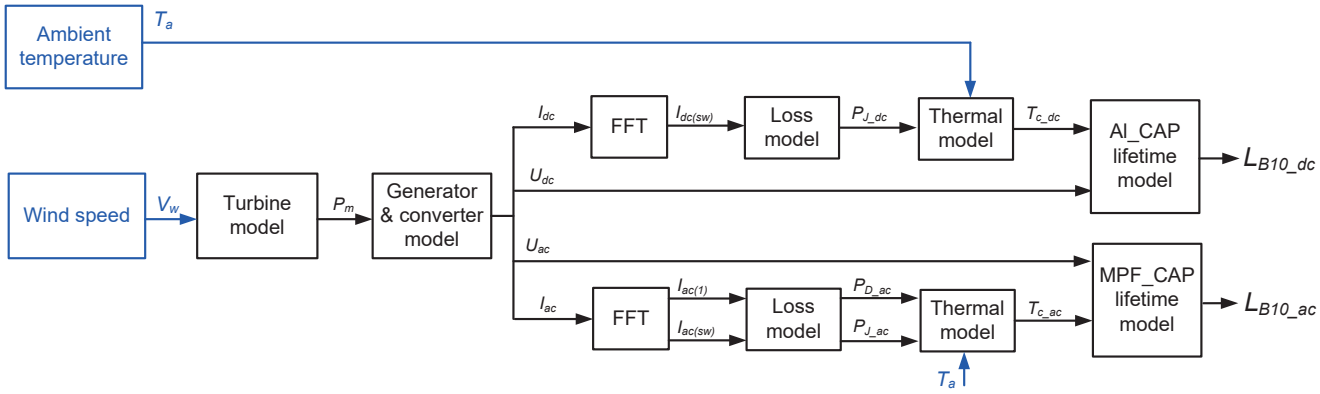

Fig. 4. Flowchart to calculate B_{10} lifetime from mission profile.

Table II

PARAMETERS RELATED TO CORE TEMPERATURE ESTIMATION OF THE USED CAPACITORS

	DC capacitor	AC capacitor
ESR	31 mΩ	2.7 mΩ
Thermal resistance from core to case	3.26 ºC/W	8.9 ºC/W

The detailed relationship between the operational hour and the applied voltage is shown in Fig. 5. It is evident that the rated lifetime of MPF-CAP (100,000 hour@80ºC) is much higher than that of the Al-CAP (6,000 hour@105ºC). Moreover, the MPF-CAP is more sensitive to the applied voltage, and the lifetime decreases rapidly with the increasing applied voltage. Furthermore, the higher core temperature of the capacitor results in lower lifetime, where the lifetime becomes a half if the temperature increases 10ºC.

With the annual wind speed (Class I) and ambient temperature with the sample rated of 1 hour as shown in Fig. 6(a), the loss profile, thermal profile and the annual accumulated damage are shown in Fig. 6(b), (c), (d), respectively. With the electrical and thermal parameters of ac-side and dc-side capacitors listed in Table II, the loss

dissipation of the MPF-CAP is much smoother because of its constant current amplitude regardless of the wind speed, and the MPF-CAP is more stressed from the thermal point of view due to its higher thermal resistance. However, in respect to the annual damage, the Al-CAP is higher due to its lower rated hour to failure.

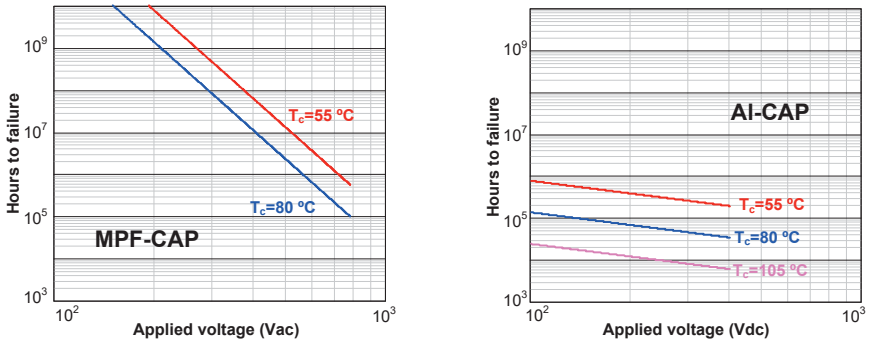

(a) (b)

Fig. 5. Hour to failure in respect to various applied voltage and various operational temperature. (a) Metalized polypropylene film capacitor; (b) Aluminum electrolytic capacitor.

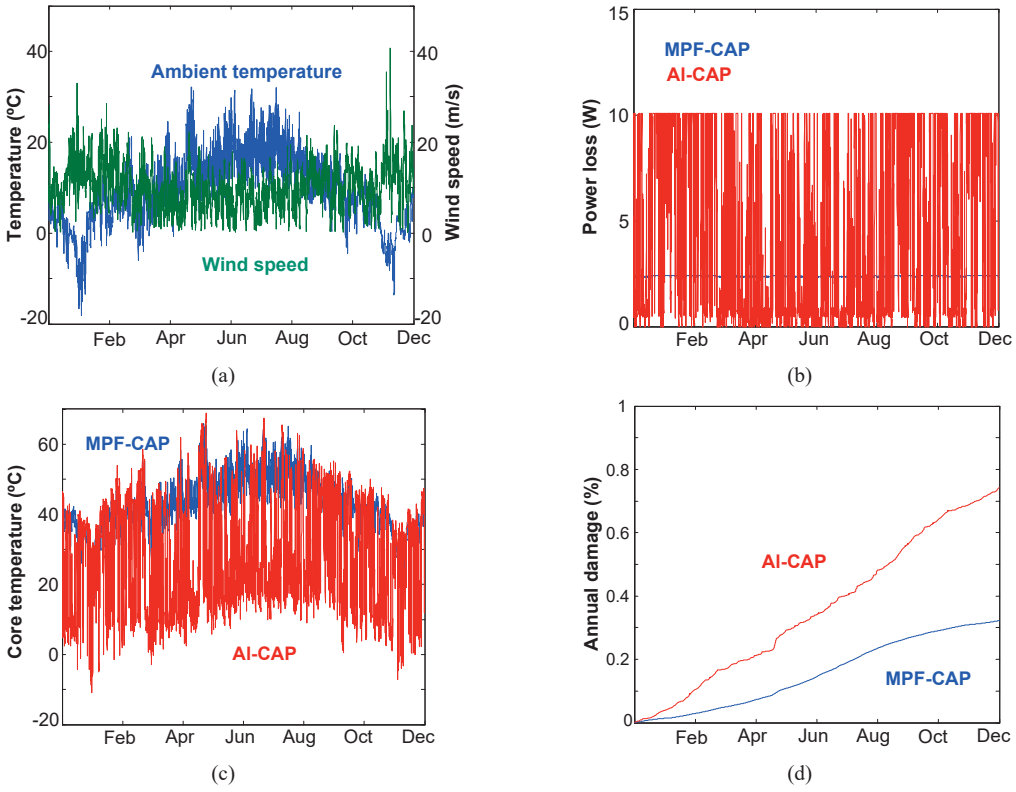

Fig. 6. Annual profile comparison between the metalized polypropylene film capacitor and the aluminum electrolytic capacitor. (a) Ambient temperature and wind speed. (b) Power loss profile. (c) Thermal stress profile. (d) Accumulated damage.

IV. Time-to-Failure of Capacitor Bank

In this section, the B_{10} lifetime of the individual capacitor can be converted into its corresponding time-to-failure. Then, the reliability evaluation of the capacitor bank can be analyzed by using the reliability block diagram.

In order to implement the accelerated degradation testing of the capacitor, the testing system is composed of a climatic chamber, a ripple current tester, and an LCR meter. Then, a degradation test is performed with a series of 9 capacitors (680 µF/63 V) at the rated voltage, rated ripple current, and upper operational temperature, where the normalized capacitance are regularly measured during 4,000 testing hours. As shown in Fig. 7(a), the degradation data is analyzed by using the software tool Reliasoft Weibull++. As the reduction rate of the capacitance increase significantly after 80% of its initial values, 20% of capacitance drop is considered as the end-of-life criteria, and the time-to-failure of each capacitor can be estimated. Presented by the Weibull, the unreliability function

is fitted in Fig. 7(b) with the shape factor β of 5.13 and the scaling factor η of 6,809.

Since the same failure mechanism has the similar failure data distribution, the shape parameter of the Weibull distribution can be assumed at 5.13 for the both Al-CAP and MPF-CAP. As any failure of the individual capacitor may result in the unreliable operation of the capacitor bank, all of the capacitors are connected in series in the reliability block diagram. The unreliability curve from the single capacitor to the capacitor bank is shown in Fig. 8. It can be seen that the lifetime of the capacitor bank is significantly reduced due to the large amount of the used capacitors. Besides, the Al-CAP bank dominates the capacitor bank lifetime. Furthermore, the expected 30-year operation only consumes the damage of 0.4%.

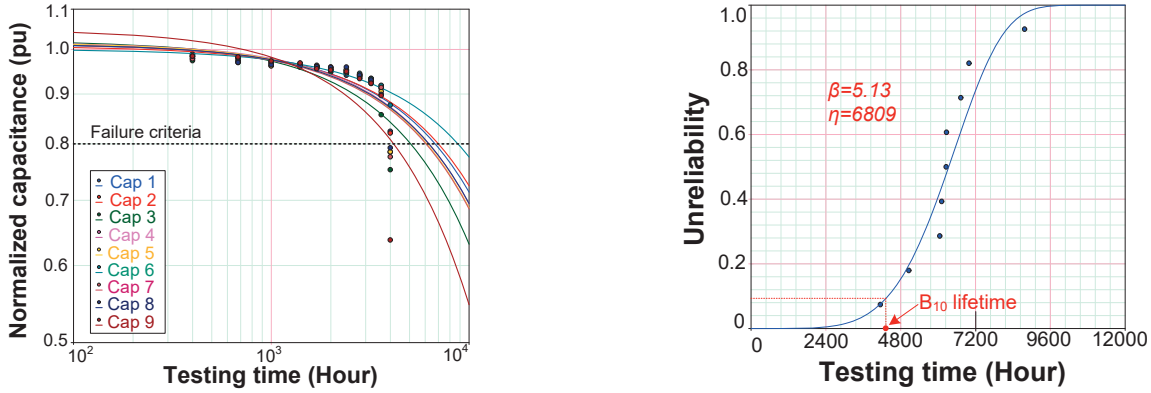

(a) (b)

Fig. 7. Degradation results for 9 capacitors at the rated voltage, rated ripple current and upper operational temperature. (a) Normalized capacitance. (b) Unreliability of capacitors along with operation time by using Weibull distribution.

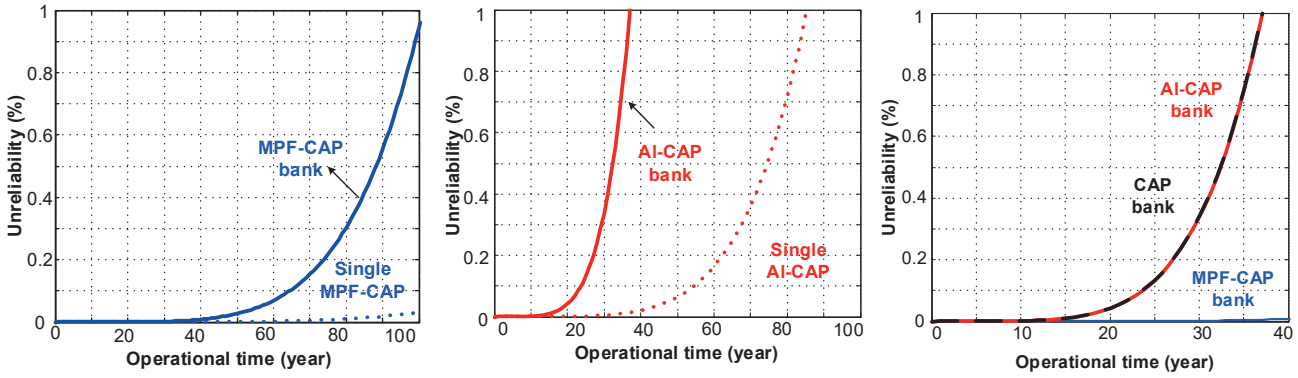

(a) (b) (c)

Fig. 8. Unreliability curve from the single capacitor to the capacitor bank. (a) Dc-side capacitor bank. (b) Ac-side capacitor bank. (c) The whole capacitor bank.

V. Conclusion

Aiming at the doubly-fed induction generator wind power generation, a reliability analysis method of power capacitor is described in this paper. It is mission profile and Weibull distribution based by investigating the long-term electro-thermal stress profile and time-to-failure distribution of the key power capacitors. A system-level reliability study of 2 MW wind turbine system is presented by the lifetime comparison between the dc-link capacitor bank and the ac-side capacitor bank. It can be concluded that the lifetime is dominated by the dc-link capacitor bank due to the lower rated lifetime of the aluminum electrolytic capacitor compared to the metalized polypropylene film capacitor.

References

[1] F. Blaabjerg, and K. Ma, "Future on power electronics for wind turbine systems," *IEEE Journal of Emerging and Selected Topics in Power Electronics*, vol. 1, no. 3, pp. 139-152, Sept. 2013.

[2] M. Liserre, R. Cardenas, M. Molinas, and J. Rodriguez, "Overview of multi-MW wind turbines and wind parks," *IEEE Trans. on Industrial Electronics*, vol. 58, no. 4, pp. 1081-1095, Apr. 2011.

[3] "ZVEI - Handbook for robustness validation of automotive electrical/electronic modules," Jun. 2013.

[4] D. Zhou, F. Blaabjerg, M. Lau, and M. Tonnes, "Optimized reactive power flow of DFIG power converters for better

reliability performance considering grid codes," *IEEE Trans. on Industrial Electronics*, vol. 62, no. 3, pp. 1552-1562, Mar. 2015.

[5] B. Sun, X. Fan, C. Qian, and G. Zhang, "PoF-simulation-assisted reliability prediction for electrolytic capacitor in LED drivers," *IEEE Trans. on Industrial Electronics*, vol. 63, no. 11, pp. 6726-6735, Nov. 2016.

[6] K. Abdennadher, P. Venet, G. Rojat, J. M. Retif, and C. Rosset, "A realtime predictive-maintenance system of aluminum electrolytic capacitors used in uninterrupted power supplies," *IEEE Trans. on Industry Applications*, vol. 46, no. 4, pp. 1644–1652, Jul. 2010.

[7] A. Lahyani, P. Venet, G. Grellet, and P. J. Viverge, "Failure prediction of electrolytic capacitors during operation of a switch-mode power supply," *IEEE Trans. on Power Electronics*, vol. 13, no. 6, pp. 1199–1207, Nov. 1998.

[8] D. Zhou, F. Blaabjerg, T. Franke, M. Tonnes, and M. Lau, "Reduced cost of reactive power in doubly fed induction generator wind turbine system with optimized grid filter," *IEEE Trans. on Power Electronics*, vol. 30, no. 10, pp. 5581-5590, Oct. 2015.

[9] H. Oh, B. Han, P. McCluskey, C. Han, and B. D. Youn, "Physics-of-failure, condition monitoring, and prognostics of insulated gate bipolar transistor modules: a review," *IEEE Trans. on Power Electronics*, vol. 30, no. 5, pp. 2413-2426, May. 2015.

[10] L. Malesani, L. Rossetto, P. Tenti, and P. Tomasin, "AC/DC/AC PWM converter with reduced energy storage in the DC link," *IEEE Trans. on Industry Applications*, vol. 31, no. 2, pp. 287-292, Mar, 1995.

[11] "Aluminum electrolytic capacitors - Capacitors with screw terminals," *EPCOS application notes*, 2007.

[12] M. Liserre, F. Blaabjerg and S. Hansen, "Design and control of an LCL-filter-based three-phase active rectifier," *IEEE Trans. on Industry Applications*, vol. 41, no. 5, pp. 1281-1291, Sep. 2005.

[13] "Aluminum Can Power Film Capacitors for PFC and AC Filter," *KEMET datasheet*, 2007

[14] Capacitor lifetime calculator. (online: http://www.illinoiscapacitor.com/tech-center/life-calculators.aspx)